IOP Publishing New J. Phys. 27 (2025) 064102 https://doi.org/10.1088/1367-2630/add496

New Journal of Physics
The open access journal at the forefront of physics

Deutsche Physikalische Gesellschaft DPG
IOP Institute of Physics

Published in partnership with: Deutsche Physikalische Gesellschaft and the Institute of Physics

OPEN ACCESS

RECEIVED
8 January 2025

REVISED
15 April 2025

ACCEPTED FOR PUBLICATION
6 May 2025

PUBLISHED
2 June 2025

PAPER

Renormalized photon propagator in quantum electrodynamics of plasmonic cavities

Marco Vallone

Dipartimento di Elettronica e Telecomunicazioni, Politecnico di Torino, corso Duca degli Abruzzi 24, 10129 Torino, Italy

E-mail: marco.vallone@polito.it

Keywords: plasmons, green's functions, cavity quantum electrodynamics, lagrangian density, coupled oscillators

Abstract

Cavity quantum electrodynamics (cQED) is a captivating field of optical physics that explores the interactions between light and matter and is particularly fascinating in the field of ultrastrong coupling. First, considering the hybridization of electromagnetic cavity (EC) modes and surface plasmon polaritons (SPPs) in a resonant cavity, we show that classical Lagrangian electrodynamics and cQED lead to the same expressions for frequency dispersion when mode dissipation and system-bath interactions are neglected. We then expand the photon propagator to a Dyson series and derive a novel non-perturbative expression for the frequency dispersion of the hybrid modes, which is equivalent to the cQED result but has a richer content. In this context, it is shown that the SPP self-interaction generates a positive self-energy that renormalizes the hybrid SPP-EC eigenfrequencies and is responsible for the well-known blue-shift of the hybrid modes, an aspect that was previously hidden in the known expressions for frequency dispersion.

1. Introduction

The study of cavity quantum electrodynamics (cQED) within the second quantization formalism provides a unique platform for exploring and understanding the interactions between light and matter [1, 2]. A prototypical case is the interaction between a two-level atomic system and a single electromagnetic cavity (EC) mode. It serves as a fundamental model in the field of quantum optics and is most simply represented by the Jaynes–Cummings model [3]. It includes the rotating wave approximation, which allows all non-resonant terms in the Hamiltonian to be neglected as they are considered minimally important [4–6].

A significant advancement is represented by the application of the Rabi quantum model [7, 8] to various physical systems, for which it has become the cornerstone of their theoretical investigation. It describes occurrences like the pairwise creation or annihilation of excitations in both atomic and photonic subsystems of high interest in nanophotonics and optoelectronics [9], the interaction of a two-level atom or a quantum dot with squeezed light [10, 11], along with interactions that involve permanent atomic electric dipole moments [12]. The likelihood of these processes increases with the light-matter coupling constant, becoming particularly relevant in the ultrastrong coupling (USC) regime, where the coupling constant approaches the energy scale of the system [13–16].

Plasmonics is an emerging and highly promising sector of quantum physics that leverages the excitations of electron density fluctuations, e.g. in semiconductor resonant cavities, excitations which are known as plasmons. The ability of plasmons to confine light within photodetectors at sub-wavelength spatial scale [12, 17] presents substantial opportunities for advances in nanophotonics and optoelectronics, including applications such as plasmon-enhanced photodetection [18–23], sensing technologies [24], and photovoltaic systems [25].

A particularly versatile type of plasmons are the surface plasmon polaritons (SPPs). They are the excitations of the oscillating local polarization density field $\mathbf{P}(\mathbf{r}, t)$ of the electron plasma, which originate from evanescent optical modes that can propagate at metallic-dielectric interfaces [26, Ch. 4], [27, 28]. In the example represented by figure 1(a), an electromagnetic plane wave determines stationary EC modes with angular frequency ω_c, described by the electric field $\mathbf{E} = \mathbf{E}_0 \exp[\mathrm{i}(\mathbf{q} \cdot \mathbf{r} - \omega_c t)]$. They may coexist with SPP

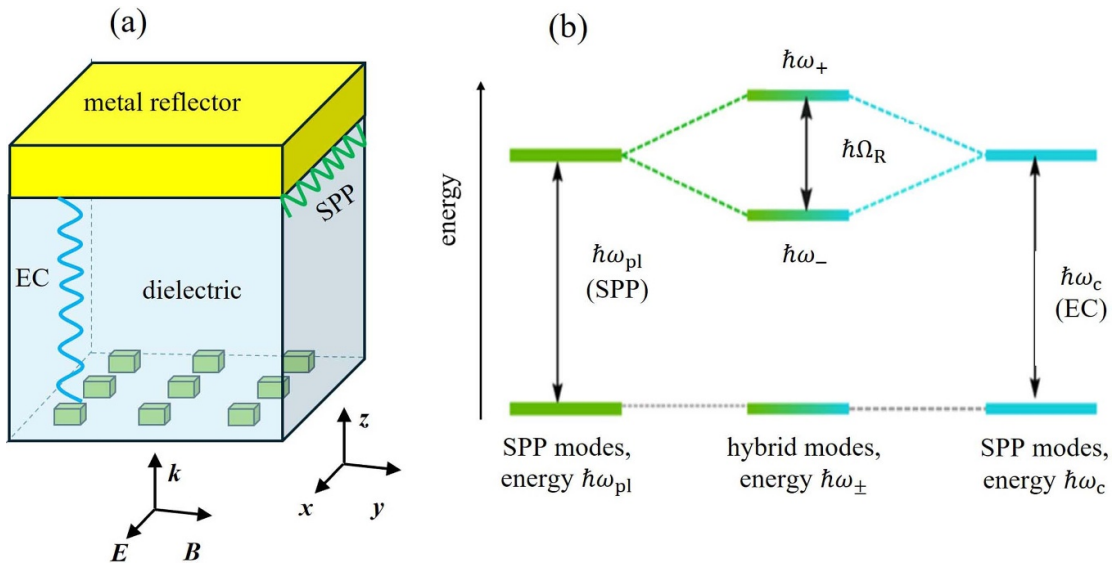

Figure 1. (a) Sketch of a resonant plasmonic cavity, illuminated at normal incidence by an electromagnetic field with polarization vector along $\hat{x}$. A lattice of metallic nanoparticles on the illuminated face excites a SPP mode [29] with electric dipole moment along $\hat{x}$ and oscillation frequency ω_{pl}. The cavity determines an EC mode with polarization vector along $\hat{x}$ and propagation vector along $\hat{z}$, which oscillates with frequency ω_c. (b) The two modes can interact to give origin to the hybrid modes $\hbar\omega_\pm$, whose separation at crossing (i.e. for $\omega_c = \omega_{pl}$) is the Rabi energy $\hbar\Omega_R$.

modes with angular frequency ω_{pl} described by $\mathbf{P} = \mathbf{P}_0 \exp[i(\mathbf{p}\cdot\mathbf{r} - \omega_{pl}t)]$. Here, $\mathbf{q}$ and $\mathbf{p}$ are the EC and SPP wavevectors, respectively, and the frequencies $\omega_{c,pl}$ are defined by the cavity details [29]. The two sets of modes can interact with a coupling coefficient $\kappa \propto \mathbf{D}\cdot\mathbf{P}$, where $\mathbf{D}$ is the electric displacement field ($\mathbf{D} = \epsilon_0\epsilon_d\mathbf{E}$, with ϵ_0 and ϵ_d the vacuum and the medium dielectric permittivity, respectively). In the weak coupling regime, the nonlinear SPP-EC interaction can be described within the classical coupled mode theory (CMT) [30–32], which leads to the two solutions

$$\omega_{\pm,\mathrm{CMT}} = \frac{\omega_c + \omega_{pl}}{2} \pm \frac{1}{2}\sqrt{\left(\omega_c - \omega_{pl}\right)^2 + 4\kappa^2}, \tag{1}$$

known as lower and upper hybrid plasmon–polaritonic branches [33]. Despite its importance, the CMT is a highly simplified representation of cavity physics, and its applicability is limited by the assumptions of weak coupling and slowly varying envelope approximation [34].

There are several excellent papers in the literature describing similar interacting systems in the context of the cQED (e.g. [17, 35, 36]), in which it is shown that the SPP-EC interaction generates hybrid modes with angular frequency $\omega_\pm$, whose functional form differs in important details from $\omega_{\pm,\mathrm{CMT}}$. However, it is often claimed in the literature, but not explicitly shown, that the same dispersion relations $\omega_\pm$ obtained by a quantum approach can also be obtained in the Lagrangian description of classical electrodynamics, provided that mode damping due to cavity dissipation and system-bath interactions, which are typical for open systems, are neglected [4, 37].

To show this important point, in section 2 we employ the Lagrangian of classical electrodynamics in the Power–Zienau–Woolley (PZW) picture $\mathcal{L}_{PZW}$ [38–44] to describe the SPP-EC coupling, obtaining the dispersion relations $\omega_\pm$ from the Euler–Lagrange equations. We emphasize that an explicit derivation of $\omega_\pm$ in Lagrangian classical electrodynamics cannot be found in the literature.

Then, in section 3 we address the same problem within the cQED, showing that, by second-quantizing the fields $\mathbf{D}$ and $\mathbf{P}$, the diagonalization of the quantum Hamiltonian resulting from $\mathcal{L}_{PZW}$ leads to the same functional forms for $\omega_\pm$ as in the classical Lagrangian formalism. Since this paper aims to be self-contained, we give an explicit yet brief derivation even of parts normally found in textbooks, as the quantization of the free fields.

The main topic of the present work, not addressed in the literature in this form, concerns the blue-shift of the hybrid modes $\omega_\pm$, which increases for both frequencies when the SPP-EC coupling strength is increased. Although the cQED correctly attributes this shift to the self-coupling of SPPs, the blue-shift of $\omega_\pm$ is not clearly singled-out from the simple mode splitting that follows from the SPP-EC avoided-crossing behavior (close energy levels repel each other as a function of some parameter, e.g. in the present case, the coupling strength).

We address this point in section 4, where a non-perturbative description of the renormalized photon propagator in plasmonic cavity is given. In short, the probability amplitude that the system is still in its ground state $|0\rangle$, after we create a photon at y and later annihilate it at x, is described by the propagator $D_{\mu\nu}(x,y) = \langle 0|\mathrm{T}\hat{A}_\mu(x)\hat{A}^\dagger_\nu(y)|0\rangle$, where T is the time-ordering symbol [1, 45, 46] and $\hat{A}_\mu$ is the μth component of the electromagnetic vector potential operator $\hat{\mathbf{A}}$, expanded in normal modes. $D_{\mu\nu}$ is expanded in a Dyson series of the free (non-interacting) photon propagator $D_{0,\mu\nu}$ and plasma dynamic polarizability, thus facilitating the extension of this approach to more complex scenarios. Following this approach, a new functional form for $\omega_\pm$ is found, which provides the same numerical results provided by the cQED description. However, this form explicitly identifies a blue-shift that is added to the frequency of the modes obtained without keeping into account the SPP self-coupling. It is described as a self-energy gained by hybrid modes propagating in a dense, self-interacting electron plasma. Finally, section 5 encapsulates the principal findings.

Regarding the notational framework, this work defines $V^\alpha = (V^0, \mathbf{V})$ and $V_\beta = (V_0, -\mathbf{V})$ as contravariant and covariant four-vectors, respectively. The Greek indices $\alpha, \beta, \mu, \ldots = 0, \ldots 3$ are employed to indicate space-time coordinates under a flat metric $g_{\mu\nu} = \mathrm{diag}(+1, -1, -1, -1)$. In contrast, Latin indices $(i, j, k, \ldots = 1, 2, 3)$ refer to the spatial components of vectors and tensors, while the not-italicized "i" is the imaginary unit. The Einstein convention to sum over repeated indices is applied. The notation $\partial/\partial x^\mu = \partial_\mu$ represents the partial derivative, with its components expressed as $(1/c\partial_t, \partial_k) = (1/c\partial_t, \nabla)$, while $\partial/\partial x_\mu = \partial^\mu = (1/c\partial_t, -\nabla)$ and $\nabla^2 = \partial_\mu\partial^\mu$.

2. Light-matter coupling: classical Lagrangian formalism

The focus of this section is the formulation of the PZW Lagrangian functional, which necessitates significant effort. Nonetheless, this step is essential for advancing towards a description of the plasmonic cavity within the cQED framework, as the latter requires the quantization of the classical Hamiltonian, which is derived from the corresponding classical Lagrangian [1, 2, 47].

2.1. The Lagrangian of nonrelativistic electrodynamics

The evolution of any physical system described by a field φ occurs as it moves from one configuration at time t_1 to another at time t_2, tracing a 'path' in the configuration space for which the action S,

$$S = \int_{t_1}^{t_2} \mathrm{d}t L(\varphi, \partial_\mu\varphi, t), \tag{2}$$

attains an extremum, most commonly a minimum: this is the principle of least action. The Lagrangian of the system $L(\varphi, \partial_\mu\varphi, t)$ defines a Lagrangian density

$$L = \int_V \mathrm{d}^3\mathbf{r}\,\mathcal{L}(\varphi, \partial_\mu\varphi, t), \tag{3}$$

that satisfies the Euler–Lagrange equations

$$\partial_\mu\left(\frac{\partial\mathcal{L}}{\partial(\partial_\mu\varphi)}\right) - \frac{\partial\mathcal{L}}{\partial\varphi} = 0. \tag{4}$$

They are the equations of motion for φ, and their solutions are stationary points of the action functional.

Starting from the electric and magnetic fields of the EC modes $\mathbf{E} = -\nabla\phi - \partial_t\mathbf{A}$ and $\mathbf{B} = \nabla\times\mathbf{A}$, respectively, written in terms of the electric scalar potential ϕ and vector potential $\mathbf{A}$ [48, ch 15], it can be shown that the classical electromagnetic Lagrangian density, in presence of an electron plasma with charge density ρ, can be written in the Lorenz gauge as (see A and [49, section 12.7])

$$\mathcal{L}_{\mathrm{em}} = \frac{\epsilon_0}{2}\left(|\partial_t\mathbf{A}|^2 - c^2|\partial_z\mathbf{A}|^2\right) - \rho\phi + \mathbf{J}\cdot\mathbf{A} \tag{5}$$

where $\mathbf{J}$ is the current density that fulfills the continuity equation $\partial_t\rho = -\nabla\cdot\mathbf{J}$. Since it is $\rho = -\nabla\cdot\mathbf{P}$ (see [2, section IV.C.1, equation (C.5)] for a derivation), it follows $\mathbf{J} = \partial_t\mathbf{P}$ and

$$\mathbf{J}\cdot\mathbf{A} = \partial_t\mathbf{P}\cdot\mathbf{A}. \tag{6}$$

We can rescale $\mathbf{P}$ to $\widetilde{\mathbf{P}} = \mathbf{P}/(\Omega_{\mathrm{pl}}\epsilon_0^{1/2})$, where Ω_{pl} is the angular plasma frequency. Then, by including the electron plasma kinetic energy density $\mathcal{T} = |\partial_t\widetilde{\mathbf{P}}|^2/2$ and writing its potential energy density $\rho\phi$ as $\omega_{\mathrm{pl}}^2|\widetilde{\mathbf{P}}|^2/2$

(see details in B), the total Lagrangian density $\mathcal{L} = \mathcal{L}_{\rm em} + \mathcal{T}$ follows as

$$\mathcal{L} = \frac{\epsilon_0}{2}\left(|\partial_t \mathbf{A}|^2 - c^2\,|\partial_z \mathbf{A}|^2\right) + \frac{1}{2}\left(\left|\partial_t \widetilde{\mathbf{P}}\right|^2 - \omega_{\rm pl}^2\left|\widetilde{\mathbf{P}}\right|^2\right) + \Omega_{\rm pl}\epsilon_0^{1/2}\,\partial_t\widetilde{\mathbf{P}}\cdot\mathbf{A}. \tag{7}$$

2.2. The PZW picture

Equation (7) contains a term proportional to **A**, which is not an observable, contrarily to its derivatives which are related to **E** and **B**. This is a very important issue, which in the literature has been addressed and solved in the dipole approximation of the multipolar gauge [50], building the PZW picture. In short, a new Lagrangian is considered, defined as $\mathcal{L} + F(t)$, where

$$F(t) = -\frac{\mathrm{d}}{\mathrm{d}t}\left(\widetilde{\mathbf{P}}\cdot\mathbf{A}\right). \tag{8}$$

It is easy to see that the resulting action $S' = \int_{t_1}^{t_2}\mathrm{d}t[\mathcal{L} + F(t)]$ is equivalent to $S = \int_{t_1}^{t_2}\mathrm{d}t\,\mathcal{L}$ in the sense that it leads to the same equations of motion, since any variation of generalized coordinates and velocities vanish at the extremal time instants. Therefore, since $\partial_t\widetilde{\mathbf{P}}\cdot\mathbf{A} + F(t) = -\widetilde{\mathbf{P}}\cdot\partial_t\mathbf{A}$, we end with the Lagrangian density

$$\mathcal{L}_{\rm PZW} = \frac{\epsilon_0}{2}\left(|\partial_t \mathbf{A}|^2 - c^2\,|\partial_z \mathbf{A}|^2\right) + \frac{1}{2}\left(\left|\partial_t \widetilde{\mathbf{P}}\right|^2 - \omega_{\rm pl}^2\left|\widetilde{\mathbf{P}}\right|^2\right) - \Omega_{\rm pl}\epsilon_0^{1/2}\,\widetilde{\mathbf{P}}\cdot\partial_t\mathbf{A}, \tag{9}$$

which contains only observable terms. Importantly, it has been shown that the PZW picture is gauge independent and leads to a quantum Hamiltonian that is fully equivalent to the more familiar Hamiltonian of the minimal-coupling picture, thus avoiding the problem of the $|\mathbf{A}|^2$ term that typically arises in minimal-coupling scenarios [35, 42, 44, 51].

2.3. Modes hybridization: dispersion relations

By plugging $\mathcal{L}_{\rm PZW}$ in the Euler–Lagrange equations, we obtain the equations of motion for **A** and $\widetilde{\mathbf{P}}$, which can be written as

$$\begin{pmatrix} \epsilon_0\left(\omega_{\rm c}^2 - \omega^2\right) & -\mathrm{i}\Omega_{\rm pl}\epsilon_0^{1/2}\omega \\ \mathrm{i}\Omega_{\rm pl}\epsilon_0^{1/2}\omega & \omega_{\rm pl}^2 - \omega^2 \end{pmatrix}\begin{pmatrix} \mathbf{A} \\ \widetilde{\mathbf{P}} \end{pmatrix} = 0, \tag{10}$$

having supposed harmonic solutions for the fields. The secular equation leads to the biquadratic equation $\left(\omega_{\rm c}^2 - \omega^2\right)\left(\omega_{\rm pl}^2 - \omega^2\right) - \Omega_{\rm pl}^2\omega^2 = 0$ whose solutions are the eigenvalues of the hybrid modes

$$\omega_\pm^2 = \frac{\omega_{\rm c}^2 + \widetilde{\omega}_{\rm pl}^2}{2} \pm \frac{\sqrt{\left(\omega_{\rm c}^2 - \widetilde{\omega}_{\rm pl}^2\right)^2 + 4\,\Omega_{\rm pl}^2\omega_{\rm c}^2}}{2}, \tag{11}$$

having defined

$$\widetilde{\omega}_{\rm pl} = \sqrt{\omega_{\rm pl}^2 + \Omega_{\rm pl}^2}. \tag{12}$$

It must be emphasized that this functional form differs significantly from the CMT description represented by equation (1) as it contains the squared frequencies. However, before commenting on the frequency dispersion $\omega_\pm$ according to the classical Lagrangian formalism and represented by equation (11), we prefer to go further and obtain the corresponding quantum formulation according to cQED.

3. Light-matter coupling: cQED formalism

The canonical quantization of a certain theory involving different fields and their possible interactions (in the present context, **A** and $\widetilde{\mathbf{P}}$) is a well-established method. It starts with a classical Lagrangian, which is a functional of the fields involved, playing the role of generalized coordinates. The conjugate momenta are then determined, leading to the formulation of the associated Hamiltonian, where fields and momenta are expressed as Fourier series. They are then elevated to the role of operators and canonical commutation relations are imposed between them. This process culminates in the formulation of the associated Hamiltonian in terms of creation and annihilation operators, which completes the quantization procedure.

The PZW Hamiltonian density is obtained from $\mathcal{L}_{\rm PZW}$ by means of the Legendre transformation

$$\mathcal{H}_{\rm PZW} = \Pi_{\mathbf{A}}\,\partial_t\mathbf{A} + \Pi_{\widetilde{\mathbf{P}}}\,\partial_t\widetilde{\mathbf{P}} - \mathcal{L}_{\rm PZW}, \tag{13}$$

where $\Pi_{\mathbf{A}}$ and $\Pi_{\widetilde{\mathbf{P}}}$ are the momenta canonically conjugate to $\mathbf{A}$ and $\widetilde{\mathbf{P}}$, respectively,

$$\Pi_{\mathbf{A}} = \frac{\partial \mathcal{L}_{\mathrm{PZW}}}{\partial\left(\partial_t \mathbf{A}\right)} = \epsilon_0 \partial_t \mathbf{A} - \sqrt{\epsilon_0}\Omega_{\mathrm{pl}}\widetilde{\mathbf{P}} = -\mathbf{D} \tag{14}$$

$$\Pi_{\widetilde{\mathbf{P}}} = \frac{\partial \mathcal{L}_{\mathrm{PZW}}}{\partial\left(\partial_t \widetilde{\mathbf{P}}\right)} = \partial_t \widetilde{\mathbf{P}}, \tag{15}$$

where for brevity we omitted their spatial and temporal dependence. Equation (14) indicates that the field velocity $\partial_t \mathbf{A}$ can be expressed as

$$\partial_t \mathbf{A} = \frac{\mathbf{P} - \mathbf{D}}{\epsilon_0}, \tag{16}$$

and the Hamiltonian density follows as

$$\begin{aligned}\mathcal{H}_{\mathrm{PZW}} = &\frac{1}{2}\left(\frac{|\mathbf{D}|^2}{\epsilon_0} + \frac{|\mathbf{B}|^2}{\mu_0}\right) + \frac{1}{2}\left(\left|\partial_t \widetilde{\mathbf{P}}\right|^2 + \omega_{\mathrm{pl}}^2\left|\widetilde{\mathbf{P}}\right|^2\right) \\ &- \frac{\Omega_{\mathrm{pl}}}{\sqrt{\epsilon_0}}\mathbf{D}\cdot\widetilde{\mathbf{P}} + \frac{\Omega_{\mathrm{pl}}^2}{2}\left|\widetilde{\mathbf{P}}\right|^2.\end{aligned} \tag{17}$$

By exploiting equations (14) and (15), since it is $|\mathbf{B}|^2 = \partial_j A^k \partial^j A_k$, the Hamiltonian density assumes the most appropriate form to be quantized:

$$\begin{aligned}\mathcal{H}_{\mathrm{PZW}} = &\frac{1}{2}\left(\frac{\Pi_{\mathbf{A}}\cdot\Pi_{\mathbf{A}}}{\epsilon_0} + \frac{\partial_j A^k \partial^j A_k}{\mu_0}\right) + \frac{1}{2}\left(\Pi_{\widetilde{\mathbf{P}}}\cdot\Pi_{\widetilde{\mathbf{P}}} + \omega_{\mathrm{pl}}^2\left|\widetilde{\mathbf{P}}\right|^2\right) \\ &+ \frac{\Omega_{\mathrm{pl}}}{\sqrt{\epsilon_0}}\Pi_{\mathbf{A}}\cdot\widetilde{\mathbf{P}} + \frac{\Omega_{\mathrm{pl}}^2}{2}\left|\widetilde{\mathbf{P}}\right|^2.\end{aligned} \tag{18}$$

The canonical quantization procedure leads to (see details in C)

$$\begin{aligned}\hat{H}_{\mathrm{PZW}} = \sum_{\mathbf{q}} \Bigg[&\underbrace{\hbar\omega_{\mathrm{c},\mathbf{q}}\left(\hat{a}_{\mathbf{q}}^{\dagger}\hat{a}_{\mathbf{q}} + \frac{1}{2}\right)}_{\hat{H}_{\mathrm{c}}} + \underbrace{\hbar\omega_{\mathrm{pl},\mathbf{q}}\left(\hat{b}_{\mathbf{q}}^{\dagger}\hat{b}_{\mathbf{q}} + \frac{1}{2}\right)}_{\hat{H}_{\mathrm{pl}}} \\ &\underbrace{-\mathrm{i}\hbar\gamma\left(\hat{a}_{\mathbf{q}} - \hat{a}_{\mathbf{q}}^{\dagger}\right)\left(\hat{b}_{-\mathbf{q}} + \hat{b}_{-\mathbf{q}}^{\dagger}\right)}_{\hat{H}_{\mathrm{int},1}} + \underbrace{\hbar\delta\left(\hat{b}_{\mathbf{q}} + \hat{b}_{\mathbf{q}}^{\dagger}\right)\left(\hat{b}_{-\mathbf{q}} + \hat{b}_{-\mathbf{q}}^{\dagger}\right)}_{\hat{H}_{\mathrm{int},2}} \Bigg],\end{aligned} \tag{19}$$

where $\hat{a}_{\mathbf{q}}^{\dagger}$ ($\hat{a}_{\mathbf{q}}$) are photon creation (annihilation) operators (and $\hat{b}_{\mathbf{q}}^{\dagger}$ ($\hat{b}_{\mathbf{q}}$) are similar operators for plasmons), and $\omega_{\mathrm{c},\mathbf{q}}$ and $\omega_{\mathrm{pl},\mathbf{q}}$ are photon and plasmon frequencies, respectively, with wavevector $\mathbf{q}$. The energy $\hbar\gamma$ plays the role of a SPP-EC coupling energy, since it couples the EC term $(\hat{a}_{\mathbf{q}} - \hat{a}_{\mathbf{q}}^{\dagger})$ and the SPP term $(\hat{b}_{-\mathbf{q}} + \hat{b}_{-\mathbf{q}}^{\dagger})$. Also $\hbar\delta$ is an energy, and it represents a SPP self-coupling term. The functional expressions of γ and δ are

$$\gamma = \frac{\Omega_{\mathrm{pl}}}{2}\sqrt{\frac{\omega_{\mathrm{c},\mathbf{q}}}{\omega_{\mathrm{pl},\mathbf{q}}}}, \quad \delta = \frac{\Omega_{\mathrm{pl}}^2}{2\omega_{\mathrm{pl},\mathbf{q}}}. \tag{20}$$

3.1. Diagonalizing the Hamiltonian

The total Hamiltonian $\hat{H}_{\mathrm{PZW}}$ is similar to the one proposed by Hopfield [52, 53] and can be diagonalized by a standard procedure.

Let us consider a EC mode $\omega_{\mathrm{c},\mathbf{q}}$ and a SPP mode $\omega_{\mathrm{pl},\mathbf{q}}$ for given wavevector $\mathbf{q}$, which can be safely omitted, for brevity. By defining a vector $\hat{v} = \left(\hat{a}\,\hat{b}\,\hat{a}^{\dagger}\,\hat{b}^{\dagger}\right)$, $\hat{H}_{\mathrm{PZW}}$ can be written as $\hat{H}_{\mathrm{PZW}} = \hat{v}^{\dagger} M \hat{v}$, where

$$M = \hbar\begin{pmatrix} \omega_{\mathrm{c}} & \mathrm{i}\gamma & 0 & \mathrm{i}\gamma \\ -\mathrm{i}\gamma & \left(\omega_{\mathrm{pl}} + \delta\right) & \mathrm{i}\gamma & \delta \\ 0 & -\mathrm{i}\gamma & \omega_{\mathrm{c}} & -\mathrm{i}\gamma \\ -\mathrm{i}\gamma & \delta & \mathrm{i}\gamma & \left(\omega_{\mathrm{pl}} + \delta\right) \end{pmatrix} \tag{21}$$

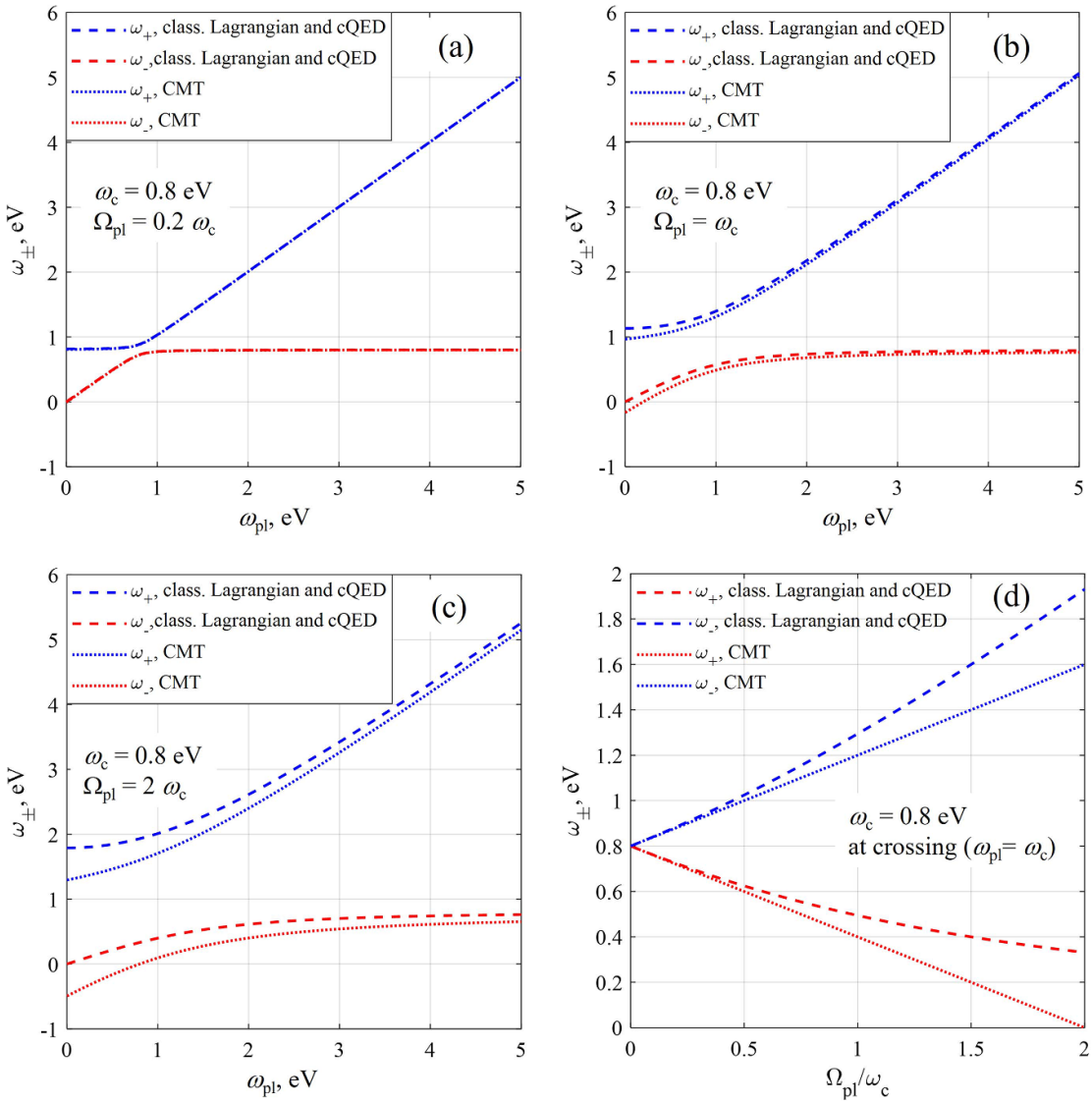

Figure 2. The eigenvalues $\omega_\pm$ (in eV) according to the classical Lagrangian formalism and cQED, compared to the simpler CMT approach, as function of the SPP energy, for $\omega_{\mathbf{q}} = 0.8$ eV (which corresponds to $\lambda = 1.55\,\mu$m). We set (a) $\Omega_{pl} = 0.2\,\omega_c$, (b) $\Omega_{pl} = \omega_c$, (c) $\Omega_{pl} = 2\,\omega_c$, while for CMT we set $\kappa = \Omega_{pl}/2$. (d) The polaritonic branches eigenfrequencies at crossing, according to the three descriptions.

can be read from $\hat{H}$. The secular equation

$$\det\left(JM - \hbar\omega\mathbb{I}\right) = 0, \tag{22}$$

where $J = \mathrm{diag}(1, 1, -1, -1)$ and $\mathbb{I}$ is the identity matrix, can be solved for ω, yielding the eigenvalues

$$\omega_\pm^2 = \frac{\omega_c^2 + \widetilde{\omega}_{pl}^2}{2} \pm \frac{\sqrt{\left(\omega_c^2 - \widetilde{\omega}_{pl}^2\right)^2 + 4\Omega_{pl}^2\omega_c^2}}{2}. \tag{23}$$

Equation (23) aligns with what we found within the classical Lagrangian framework (see equation (11)), therefore demonstrating that quantum and classical descriptions lead to the same results, in absence of damping and for closed systems. Figures 2(a)–(c) compares the results obtained according to the CMT, to the classical Lagrangian formalisms, and within the cQED description. The latter two approaches are represented by equation (23) or (11), which coincide, and all the three formalisms describe the well-known avoided-crossing behavior, typical of interacting oscillators. We notice that the CMT result progressively deviates when Ω_{pl} is increased. Moreover, figure 2(d) shows that the separation of the two hybrid modes at crossing, (i.e. when $\omega_c = \omega_{pl}$) increases quasi-linearly with Ω_{pl} according to the CMT, while this is not true in the Lagrangian and cQED descriptions, because of a frequency blue-shift. Section 4 will clarify this point. Some other considerations are in order:

- classical Lagrangian and cQED formulations, equations (11) and (23), respectively, contain and return the squares of the frequencies, unlike the description according to the CMT, equation (1);
- in the classical Lagrangian and cQED descriptions, an additional term $\Omega_{\rm pl}^2$ blue-shifts the squared plasmonic resonance $\omega_{\rm pl}^2$ to $\widetilde{\omega}_{\rm pl}^2$, the meaning of which will be better clarified in the context of the propagator formalism, section 4;
- the mode separation $|\omega_+ - \omega_-|$ reaches the minimum value for $\omega_{\rm pl} = \omega_{\rm c}$ in all the approaches. Assuming natural units ($\hbar = 1$, therefore ω is an energy, expressed in eV in all the figures) and indicating this value with δE, in the CMT it is $\delta E = 2\kappa$, while it is $\delta E = \Omega_{\rm pl}$ in the classical Lagrangian and cQED approaches.

Very importantly, it is possible to rewrite equation (23) as

$$\omega_\pm^2 = \frac{\omega_{\rm c}^2 + \widetilde{\omega}_{\rm pl}^2}{2} \pm \frac{\sqrt{\left(\omega_{\rm c}^2 + \widetilde{\omega}_{\rm pl}^2\right)^2 - 4\omega_{\rm pl}^2\omega_{\rm c}^2}}{2} \tag{24}$$

which is exactly the [36, equation (S8)] obtained by employing the full Hopfield-type Hamiltonian [53], retaining both the counter-rotating terms ($\hat{a}_{\mathbf{q}}^\dagger \hat{a}_{\mathbf{p}}^\dagger$, $\hat{a}_{\mathbf{q}}\hat{a}_{\mathbf{p}}$, $\hat{a}_{\mathbf{q}}^\dagger \hat{b}_{\mathbf{p}}^\dagger$, and $\hat{a}_{\mathbf{q}}\hat{b}_{\mathbf{p}}$) and the photon self-interaction term proportional to $|\mathbf{A}|^2 \propto (\hat{a}_{\mathbf{q}}^\dagger + \hat{a}_{-\mathbf{q}})^2$, which is typically present in the minimal-coupling approach, but absent in the PZW representation.

Some other considerations are in order. When we neglect the SPP self-coupling term $\hat{H}_{\rm int,2}$ by setting $\delta = 0$ in equation (19), the eigenvalues become

$$\omega_\pm^2 = \frac{\omega_{\rm c}^2 + \omega_{\rm pl}^2}{2} \pm \frac{1}{2}\sqrt{\left(\omega_{\rm c}^2 - \omega_{\rm pl}^2\right)^2 + 4\Omega_{\rm pl}^2\omega_{\rm c}^2} \tag{25}$$

which can be obtained from the Dicke model [52], an approximation of the Hopfield Hamiltonian that retains the counter-rotating terms, but neglects $|\mathbf{A}|^2$ (see also [36, equation (S9)]). Equation (25) does not feature any frequency blue-shift, which therefore can be ascribed to the SPP self-interactions.

Furthermore, by neglecting both the $\hat{H}_{\rm int,2}$ term *and* the counter-rotating terms in our Hamiltonian, i.e. $\hat{b}_{\mathbf{q}}^\dagger \hat{a}_{\mathbf{q}}^\dagger$, $\hat{a}_{\mathbf{q}}^\dagger \hat{b}_{\mathbf{q}}^\dagger$, $\hat{b}_{\mathbf{q}}\hat{a}_{\mathbf{q}}$ and $\hat{a}_{\mathbf{q}}\hat{b}_{\mathbf{q}}$, the matrix M decouples and the eigenvalues take the same form as in the simple CMT (where the frequencies are not squared)-

$$\omega_\pm = \frac{\omega_{\rm c} + \omega_{\rm pl}}{2} \pm \frac{1}{2}\sqrt{\left(\omega_{\rm c} - \omega_{\rm pl}\right)^2 + 4\gamma^2}. \tag{26}$$

In few words, it is noticeable the ability of the cQED approach to provide a clear meaning also for the approximated results coming from the CMT.

As a final note, it seems that there is no immediate benefit coming from the cQED approach, since it leads to the same result obtained in classical Lagrangian electrodynamics. The correct answer can be given by examining in what cases the classical approach fails. In general, the cQED is unavoidable whenever a given process generates or absorbs new frequencies of radiation, as for the spontaneous emission and in open-systems. In the other cases, the classical formalism is seemingly sufficient. However, this is not the whole story.

4. The propagator formalism for the SPP-EC interaction

A crucial unresolved question is the origin of the blue-shift visible in figure 2(d). Although the cQED Hamiltonian includes SPP self-interaction, its eigenvalues at the crossing (equation (23) with $\omega_{\rm c} = \omega_{\rm pl}$) are not expressed as the free photon energy $\omega_{\rm c}$, shifted by the SPP-EC coupling frequency $\pm\gamma$, plus a blue-shift Σ (a correction) due to the SPP self-interaction: $\omega_\pm = \omega_{\rm c} \pm \gamma + \Sigma$. Equation (23) has a very different form, and the correction Σ is somehow embedded in the description but not singled out and summed to the other terms.

The propagator theory is a powerful way to address this issue and allows to develop a non-perturbative theory that accounts for light-matter strong-coupling. If we were in vacuum, the retarded Green's function (propagator) of the photon would be

$$\Delta_{0,\mu\nu}^+(x-y) = \langle 0|\mathrm{T}\hat{A}_\mu(x)\hat{A}_\nu^\dagger(y)|0\rangle. \tag{27}$$

It describes a free, non-interacting photon created in y and destroyed at a later time in x. Here, $\hat{A}_\mu(x)$ is the vector potential operator

$$\hat{A}_\mu(x) = \sum_{\mathbf{k}} \sum_{\lambda=1}^{3} \xi_\mu^\lambda \sqrt{\frac{\hbar}{2\epsilon_0 \omega_{\mathbf{k}}}} \left(\hat{a}_{\mathbf{k}} e^{-ikx} + \hat{a}_{\mathbf{k}}^\dagger e^{ikx} \right) \tag{28}$$

expanded in normal modes, where ξ_μ^λ is the polarization three-vector. Following [1, ch. 9], $\Delta_{0,\mu\nu}^+(x-y)$ can be written in the Feynman's gauge and in the momentum space as

$$\Delta_{0,\mu\nu}^+(\omega, \mathbf{k}) = i \frac{g_{\mu\nu}}{\omega_{\mathbf{k}}^2 - \omega^2 + i\eta}, \tag{29}$$

where the positively definite infinitesimal η provides the correct causality prescription.

Concerning the case under study, we are considering a different scenario: an optical cavity filled with uniform, nonmagnetic electron plasma with refractive index $n = \sqrt{\epsilon_d}$. To find an explicit form for the photon propagator, we consider time harmonic classical fields with $e^{-i\omega t}$ dependence. From the Maxwell–Faraday equation $\nabla \times \mathbf{E} = i\omega \mathbf{B}$ and the Ampère-Maxwell equation $\nabla \times \mathbf{B} = \mu_0 (\mathbf{J} - i\omega \epsilon_0 \epsilon_d \mathbf{E})$, and recalling that $\mathbf{J}$ and $\mathbf{P}$ are related by (see section 2.1) $\mathbf{J} = \partial_t \mathbf{P} = -i\omega \mathbf{P}$, in natural units (light velocity $c = 1$) we have

$$\nabla \times \nabla \times \mathbf{E} = \omega^2 \mu_0 \mathbf{P} + n^2 \omega^2 \mathbf{E}, \tag{30}$$

which can be written as

$$\left(-\nabla^2 - n^2 \omega^2 \right) \mathbf{E} = \omega^2 \mu_0 \mathbf{P}. \tag{31}$$

The Green's function $D_{0,ij}$ associated to the differential operator in the LHS of equation (31) is the solution of

$$\left(-\nabla^2 - n^2 \omega^2 \right) D_{0,ij}(\omega, \mathbf{r} - \mathbf{r}') = n^2 \omega^2 \delta(\mathbf{r} - \mathbf{r}') \delta_{ij}, \tag{32}$$

where δ_{ij} is the Kronecker-δ. Now we express $D_{0,ij}(\omega, \mathbf{r} - \mathbf{r}')$ and the Dirac-δ as Fourier transforms,

$$D_{0,ij}(\omega, \mathbf{r} - \mathbf{r}') = \int \frac{d^3\mathbf{k}}{(2\pi)^3} e^{i\mathbf{k}\cdot(\mathbf{r}-\mathbf{r}')} D_{0,ij}(\omega, \mathbf{k}) \tag{33}$$

$$\delta(\mathbf{r} - \mathbf{r}') = \int \frac{d^3\mathbf{k}}{(2\pi)^3} e^{i\mathbf{k}\cdot(\mathbf{r}-\mathbf{r}')}, \tag{34}$$

which, when plugged in equation (32) keeping into account that in natural units it is $|\mathbf{k}|^2 = n^2 \omega_{\mathbf{k}}^2$, they lead to

$$D_{0,ij}(\omega, \mathbf{k}) = \delta_{ij} \frac{\omega^2}{\omega_{\mathbf{k}}^2 - \omega^2}. \tag{35}$$

(We omitted the infinitesimal $i\eta$, which is unnecessary for the description which follows).

In the language typical of the physics of condensed matter [54], 'bare' particles are effectively 'dressed' with virtual particles because of the interactions that transform them into physical particles, the only ones that can be observed. In a plasmonic cavity, the properties of the free, 'bare' photon propagator $D_{0,ij}$ are not observable, since the cavity photons are not 'bare'. The photon propagator corresponding to the observable field excitations is called 'dressed'. We can call it D_{ij} and imagine that it describes a bare photon that decays into a bubble of plasma dipole excitations (plasmons) π_{ij} during propagation, which immediately transforms back into a bare photon. Considering a Dyson series of these possibilities, we can write D_{ij} as

$$D_{ij} = D_{0,ij} + D_{0,ik}\pi^{kl}D_{0,jl} + D_{0,ik}\pi^{kl}D_{0,lm}\pi^{mn}D_{0,jn} + \ldots = D_{0,ij} + D_{0,im}\pi^{mn}D_{jn}. \tag{36}$$

$D_{0,ij}$ is a tensorial quantity, but when in the cavity there is a dominant EC mode with frequency $\omega_{\mathbf{k}} = \omega_c$, definite transverse polarization and propagation vector along a given direction, $D_{0,ij}$ can be written more simply in the frequency domain as the scalar quantity

$$D_0(\omega) = \frac{\omega^2}{\omega_c^2 - \omega^2}. \tag{37}$$

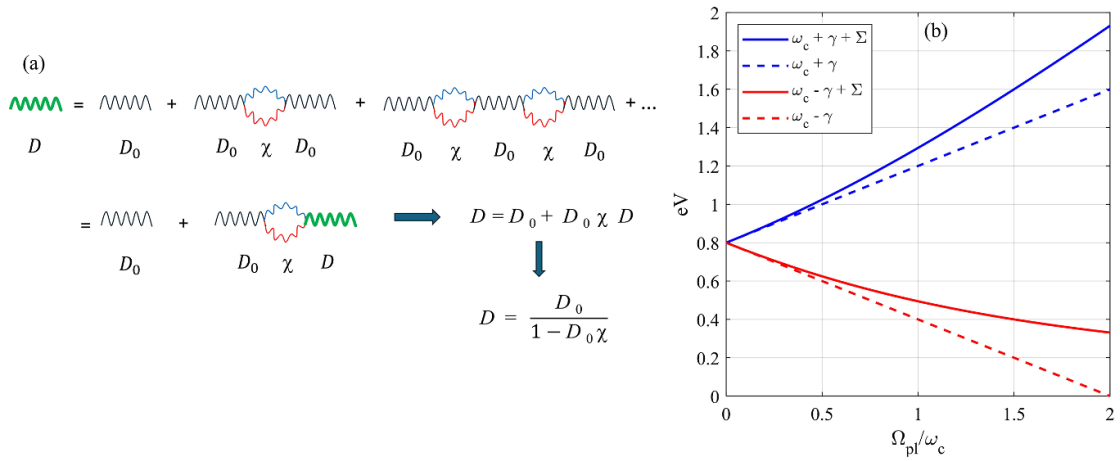

Figure 3. (a) Graphical representation of the Dyson's equation for the cavity photon dressed propagator D. (b) The polaritonic branches eigenfrequencies at crossing, according to $\omega_{\pm} = \omega_c \pm \gamma$ and to $\omega_{\pm} = \omega_c \pm \gamma + \Sigma$.

With this simplification, also the plasma dipole excitation π_{ij} becomes a scalar quantity, the electric susceptibility χ, and the Dyson series becomes

$$D = D_0 + D_0\chi D_0 + D_0\chi\Delta_0\chi D_0 + \ldots = D_0 + D_0\chi D \tag{38}$$

from which it follows

$$D = \frac{D_0}{1 - D_0\chi}, \tag{39}$$

graphically illustrated in figure 3(a).

The electric susceptibility relates the local polarization density $\mathbf{P}$ to the local electric field distribution $\mathbf{E}$ according to $\mathbf{P} = \epsilon_0\chi\mathbf{E}$. It must be kept in mind that the electric susceptibility is a macroscopic quantity connected to the microscopic dynamic polarizability of the plasma α via the local electron density n_0 according to $\chi = n_0\alpha$. A widely adopted expression for χ is the Lorentz model

$$\chi(\omega) = \frac{\Omega_{\mathrm{pl}}^2}{\omega_{\mathrm{pl}}^2 - \omega^2}. \tag{40}$$

It describes the excitation of an elementary oscillator with natural frequency ω_{pl} and, in this form, without damping. By plugging the expressions for D_0 and χ in the equation (39), we obtain

$$D = \frac{\omega^2\left(\omega_{\mathrm{pl}}^2 - \omega^2\right)}{\left(\omega_c^2 - \omega^2\right)\left(\omega_{\mathrm{pl}}^2 - \omega^2\right) - \omega^2\Omega_{\mathrm{pl}}^2}. \tag{41}$$

The eigenfrequencies of the response function coincide with the position of the poles of D, which are given by

$$\omega_{\pm}^2 = \frac{\omega_c^2 + \widetilde{\omega}_{\mathrm{pl}}^2}{2} \pm \frac{\sqrt{\left(\omega_c^2 - \widetilde{\omega}_{\mathrm{pl}}^2\right)^2 + 4\Omega_{\mathrm{pl}}^2\omega_c^2}}{2}. \tag{42}$$

This form aligns with the equation (23), which was derived in the second quantization formalism. However, the concept of self-energy, which is explicitly defined in the Dyson series, leads to separate a shift $\pm\gamma$, which describes the anti-crossing behavior between the SPP and EC modes, from an additional shift Σ, which results from the SPP self-interaction and represents a positive self-energy which blue-shifts both eigenfrequencies,

$$\omega_{\pm} = \omega_c \pm \gamma + \Sigma. \tag{43}$$

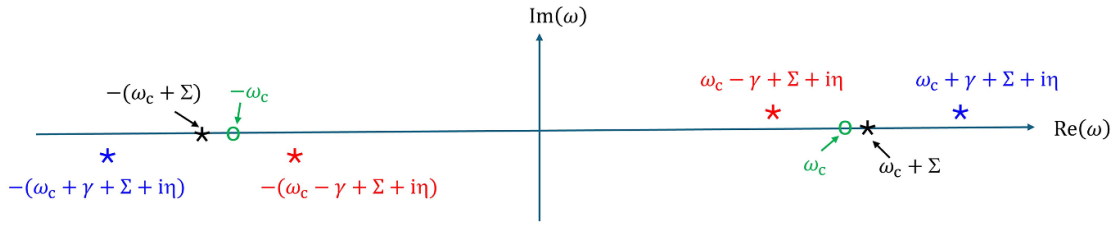

Figure 4. Poles structure of the propagator $D(\omega)$ in the frequency complex plane.

To retrieve these contributions, we first recognize that the denominator of D is a quartic polynomial characterized by two positive roots, denoted as $\omega_\pm$, and two negative roots, $-\omega_\pm$. Consequently, we can write it as

$$\left(\omega_c^2-\omega^2\right)\left(\omega_{pl}^2-\omega^2\right)-\omega^2\Omega_{pl}^2=\left(\omega-\omega_+\right)\left(\omega-\omega_-\right)\left(\omega+\omega_+\right)\left(\omega+\omega_-\right). \tag{44}$$

Then, we equate the coefficients of the two polynomials in the last equation, expressing $\omega_\pm$ according to equation (43). At the crossing (i.e. for $\omega_{pl}=\omega_c$) we find the expressions for the separation between the polaritonic branches 2γ and the self-energy Σ as

$$\gamma=\frac{\Omega_{pl}}{2} \tag{45}$$

$$\Sigma=\omega_c\left(\frac{\sqrt{t^2+4}}{2}-1\right), \tag{46}$$

having defined $t=\Omega_{pl}/\omega_c$. It is important to note that Σ is a positive correction to the eigenvalues $\omega_c\pm\gamma$, therefore it plays the role of a self-energy.

In figure 3(b) we show the photon eigenfrequencies in the cavity, represented by (bare solutions) $\omega_\pm=\omega_c\pm\gamma$ and (dressed solutions) $\omega_\pm=\omega_c\pm\gamma+\Sigma$. The results derived from the latter expression are totally equivalent to those depicted in figure 2(d).

The propagator D can be expressed more effectively by separating the contributions coming from the four poles, now including again the positive infinitesimal η. As shown in figure 4, two poles represent the positive solutions $\omega_\pm$ and lie in the frequency upper complex plane. The other two poles correspond to the negative solutions $-\omega_\pm$ and lie in the lower complex plane,

$$D(\omega)=A_1\frac{1}{\omega-(\omega_c+\gamma+\Sigma+i\eta)}+A_2\frac{1}{\omega-(\omega_c-\gamma+\Sigma+i\eta)}+[\text{neg. sol.}], \tag{47}$$

where $A_1=0.5(\omega_+^2-\omega_{pl}^2)/(\omega_+-\omega_-)$ and $A_2=0.5(\omega_{pl}^2-\omega_-^2)/(\omega_+-\omega_-)$.

In this formulation, the role of the self-energy Σ is better evident as a blue-shift, a renormalization of the propagator poles, and it is an effect whose origin lies in the interaction of EC and SPP oscillators, and operate even in a classical context.

4.1. Processes in the USC regime

The validation of equation (23) using numerical simulations or experimental data, if available, would represent an important point. In some recent works [29, 55], the cQED description was applied to a realistic plasmonic cavity, specifically a photodetector operating in the mid-infrared band, $\lambda\in[3,5]\,\mu$m. Its electro-optical response was investigated by numerical simulations using the finite differences time domain (FDTD) method, in which the electronic transport and Maxwell equations were solved after the detector was discretized on a three-dimensional grid. The cited references show that the FDTD numerical simulations reproduce the SPP-EC anti-crossing behavior described in the present work. In spite of this, the two polaritonic branches are symmetrical, so no blue-shift is detected.

The full Hamiltonian $\hat{H}_{PZW}$ is nonlinear, and the Dyson's expansion of the photon propagator yields a self-energy that describes the nonlinear interactions between the photon and the plasma. As a result, numerical FDTD simulations (which include linear interactions only) cannot predict any blue-shift. Specifically, they are expected to confirm the overall scenario only within the regime described by equation (26), which is obtained by neglecting both the $\hat{H}_{int,2}$ term *and* the counter-rotating terms in the Hamiltonian. The same result is equivalently provided by equation (43) after setting $\Sigma=0$, which, however, has little meaning. In fact, the cited [29, 55] show γ and ω_c to have a comparable order of magnitude, which

drives the physical system under consideration into the regime of so-called USC. Therefore, a description neglecting the photon self-energy (as in standard electro-optical FDTD simulations) is only a rough approximation, and the experimental wavelength of the polaritonic branches could deviate because of the blue-shift due to the contribution of Σ. Moreover, it must be pointed out that in the USC regime higher order transitions and multi-photon processes become relevant. A good theoretical and experimental description can be found in [56], and the blue-shift is well visible in experimental works [16, 57, 58].

The USC regime is particularly interesting for two-levels or multi-level systems [14, 35, 59–62], nanoparticle crystals [16, 36] or spin-boson systems [63] coupled to a plasmonic cavity. Good reviews and contributions on these topics can be found e.g. in [15, 17, 23, 58], where the USC regime, its relation to the weak coupling regime and other regimes that compare γ with the plasmon lifetime determined by the losses, are described in detail.

The interaction representation of the Hamiltonian, which provides the Dyson equation for D, also leads to a description of multiphoton and other higher order processes. For example, in the USC regime an array of nanoparticles may exhibits two-photon absorption associated with Kerr nonlinearity [64, 65], saturation and reverse saturation of scattering [66], plasmon-exciton interactions [67]. Furthermore, the formation and dynamics of spin-glass [68] can be described at a level between statistical physics and quantum field theory by the application of the nonequilibrium Dyson equations in the USC regime. Specifically, a quantum effective action for the system can be expressed as a function of its two-point correlation functions, leading to a description of the dynamics of the system, by means of some controlled non-perturbative approximations [69, 70].

5. Conclusions and future work

In this contribution we describe the interactions between cavity electromagnetic modes and SPPs. To this end, we present the explicit derivation of the frequency dispersion relations in the classical Lagrangian electrodynamics and by following the second quantization formalism, demonstrating the equivalency of quantum and classic approaches, in case the modes damping due to cavity dissipation and system-bath interactions typical of open-systems can be neglected. This conclusion is expected and claimed in the literature, but not explicitly given, at the best of author's knowledge.

By employing a Dyson series expansion of the photon propagator within a resonant plasmonic cavity, we derive an alternative yet equivalent formulation for frequency dispersion. In this framework, the self-interaction of plasmons is demonstrated to establish a positive self-energy, resulting in a blue-shift of the eigenfrequencies associated with the hybrid photon–plasmon modes. This phenomenon was previously obscured in the original expressions for frequency dispersion.

The inclusion of cavity dissipation and system-bath interactions within the SPP-EC interactions treated by the propagator formalism is ongoing and will be the object of a separate contribution.

Data availability statement

All data that support the findings of this study are included within the article (and any supplementary files).

Appendix A. Classical electromagnetic Lagrangian

Let us start from the Maxwell equations in presence of charges and currents and consider a non-magnetic material,

$$\nabla \cdot \mathbf{E} = \frac{\rho}{\epsilon_0} \tag{A.1}$$

$$\nabla \cdot \mathbf{B} = 0 \tag{A.2}$$

$$\nabla \times \mathbf{E} = -\partial_t \mathbf{B} \tag{A.3}$$

$$\nabla \times \mathbf{B} = \mu_0 \mathbf{J} + \frac{1}{c^2}\partial_t \mathbf{E}. \tag{A.4}$$

Here $\mathbf{J}$ is the electrical current, ρ is the free charge density, and μ_0 is the vacuum magnetic permeability (the magnetic permeability of the dielectric is $\mu = 1$, since the material is considered non-magnetic).

The electric and magnetic fields $\mathbf{E}$ and $\mathbf{B}$ can be expressed in terms of the electromagnetic four-potential

$$A^\mu = \left(\frac{\phi}{c}, \mathbf{A}\right) \tag{A.5}$$

as [48, Chapter 15]

$$\begin{aligned}\mathbf{E} &= -\nabla\phi - \partial_t \mathbf{A}\\ \mathbf{B} &= \nabla \times \mathbf{A},\end{aligned} \tag{A.6}$$

where ϕ is the electric scalar potential and $\mathbf{A}$ is the vector potential. With reference to the geometry described in figure 1, $\mathbf{A}$ is parallel to $\mathbf{E} = (E, 0, 0)$, and it is $\mathbf{B} = (0, B, 0)$.

We can define a four-current $j^\mu = (c\rho, \mathbf{J})$, write the continuity equation as $\partial_\mu j^\mu = 0$, and build the second-rank antisymmetric electromagnetic tensor $F_{\mu\nu}$ as $F_{\mu\nu} = \partial_\mu A_\nu - \partial_\nu A_\mu$. To simplify the equations which follow without loosing generality, it is customary to exploit the gauge freedom, imposing the Lorenz gauge [48, chapter 15] $\partial_\mu A^\mu = 0$.

The equation $\partial_\mu F^{\mu\nu} = \mu_0 j^\nu$ provides the Maxwell equations equation (A.1) and equation (A.4) for $\nu = 0$ and $\nu = k$, respectively. In the Lorenz gauge, this equation simplifies to

$$\partial_\mu \partial^\mu A^\nu = \mu_0 j^\nu, \tag{A.7}$$

that is the equation of motion for the field A^ν. Importantly, the latter can be obtained from the Euler–Lagrange equations, equation (4), starting from the electromagnetic Lagrangian density

$$\mathcal{L}_{\text{em}} = -\frac{1}{4\mu_0} F_{\mu\nu} F^{\mu\nu} - j_\mu A^\mu, \tag{A.8}$$

where $j_\mu A^\mu = \rho\phi - \mathbf{J}\cdot\mathbf{A}$ is the source term. Therefore it is

$$\mathcal{L}_{\text{em}} = \frac{\epsilon_0}{2}\left(|\partial_t \mathbf{A}|^2 - c^2 |\partial_z \mathbf{A}|^2\right) - \rho\phi + \mathbf{J}\cdot\mathbf{A}. \tag{A.9}$$

Appendix B. Plasmons classical Lagrangian

The free electrons in the cavity can oscillate with frequency ω_{pl} around their equilibrium position, e.g. following the surface electromagnetic wave that, if excited [29], can propagate along the dielectric/metal interface of the cavity. The displacement $\mathbf{q}_k(t)$ of the kth free electron can be replaced in the continuum limit by $\mathrm{d}^3\mathbf{r}\, n_0\, \mathbf{q}(\mathbf{r}, t)$, where $\mathbf{q}(\mathbf{r}, t)$ is a continuous function, the infinitesimal volume $\mathrm{d}^3\mathbf{r}$ contains $n_0 \mathrm{d}^3\mathbf{r}$ electrons, n_0 being the average electron number density in the dielectric. Differentiating, we obtain the electrons velocity as $\dot{\mathbf{q}}_k(t) \to \mathrm{d}^3\mathbf{r}\, n_0\, \dot{\mathbf{q}}(\mathbf{r}, t)$ and its square as $|\dot{\mathbf{q}}_k(t)|^2 \to \mathrm{d}^3\mathbf{r}\, n_0\, |\dot{\mathbf{q}}(\mathbf{r}, t)|^2$.

In this way, we can write the distribution of the electric dipole moment in the dielectric as $e\mathbf{q}(\mathbf{r}, t)$, where e is the electron charge, and the distribution of the electric dipole moment density as $\mathbf{P}(\mathbf{r}, t) = n_0 e \mathbf{q}(\mathbf{r}, t)$. When differentiated and squared, it yields

$$|\dot{\mathbf{q}}(\mathbf{r}, t)|^2 = \left|\frac{\partial_t \mathbf{P}(\mathbf{r}, t)}{e n_0}\right|^2, \tag{B.1}$$

from which the total kinetic energy T of the plasma follows as

$$\begin{aligned}T(t) &= \frac{m_{\text{e}}}{2}\sum_k |\dot{\mathbf{q}}_k(t)|^2\\ &\to \frac{m_{\text{e}}}{2 e^2 n_0}\int_V \mathrm{d}^3\mathbf{r}\, |\partial_t \mathbf{P}(\mathbf{r}, t)|^2\end{aligned} \tag{B.2}$$

and its density $\mathcal{T}(\mathbf{r}, t)$ as

$$\mathcal{T}(\mathbf{r}, t) = \frac{1}{2\epsilon_0 \Omega_{\text{pl}}^2} |\partial_t \mathbf{P}(\mathbf{r}, t)|^2, \tag{B.3}$$

where m_{e} is the effective electron mass and $\Omega_{\text{pl}} = \sqrt{e^2 n_0/(m_{\text{e}}\epsilon_0)}$ is the plasma frequency.

The kth electron, when it moves away from its equilibrium position, gains a potential energy

$$U(t) = \frac{1}{2} m_{\text{e}} \omega_{\text{pl}}^2 \sum_k |\mathbf{q}_k(t)|^2, \tag{B.4}$$

which can be written in the continuous limit as

$$U(t) = \frac{m_e}{2}\omega_{pl}^2 \int_V d^3\mathbf{r}\, n_0 \left|\frac{\mathbf{P}(\mathbf{r},t)}{e n_0}\right|^2 = \frac{\omega_{pl}^2}{2\epsilon_0 \Omega_{pl}^2}\int_V d^3\mathbf{r}\, |\mathbf{P}(\mathbf{r},t)|^2, \tag{B.5}$$

and defines the potential energy density as

$$\mathcal{U}(\mathbf{r},t) = \frac{\omega_{pl}^2}{2\epsilon_0\Omega_{pl}^2}|\mathbf{P}(\mathbf{r},t)|^2. \tag{B.6}$$

The Lagrangian density of the SPP plasmonic mode follows as

$$\begin{aligned}\mathcal{L}_{pl} &= \mathcal{T}(\mathbf{r},t) - \mathcal{U}(\mathbf{r},t)\\ &= \frac{1}{2\epsilon_0\Omega_{pl}^2}\left(|\partial_t \mathbf{P}(\mathbf{r},t)|^2 - \omega_{pl}^2|\mathbf{P}(\mathbf{r},t)|^2\right)\\ &= \frac{1}{2}\left(\left|\partial_t \widetilde{\mathbf{P}}(\mathbf{r},t)\right|^2 - \omega_{pl}^2\left|\widetilde{\mathbf{P}}(\mathbf{r},t)\right|^2\right)\end{aligned} \tag{B.7}$$

having rescaled **P** to

$$\widetilde{\mathbf{P}} = \frac{\mathbf{P}}{\Omega_{pl}\epsilon_0^{1/2}}. \tag{B.8}$$

Appendix C. Canonical quantization of fields and Hamiltonian

The canonical quantization procedure includes the expansion of the fields into Fourier series. Then, by elevating the latters to the role of operators, their quantization, obtained by imposing canonical commutation relations between fields and momenta, leads to the definition of creation and annihilation operators, through which photons and plasmons appear as excitations of the involved fields.

C.1. Fields expansion

The first step is the expansion of the fields **A**, $\widetilde{\mathbf{P}}$, $\Pi_{\mathbf{A}}$ and $\Pi_{\widetilde{\mathbf{P}}}$ which appear in the PZW Hamiltonian, equation (18), into Fourier series,

$$\begin{aligned}\widetilde{\mathbf{P}}(\mathbf{r},t) &= \frac{1}{\sqrt{V}}\sum_{\mathbf{p}} e^{i\mathbf{p}\cdot\mathbf{r}}\widetilde{\mathbf{P}}_{\mathbf{p}}(t)\\ \Pi_{\widetilde{\mathbf{P}}}(\mathbf{r},t) &= \frac{1}{\sqrt{V}}\sum_{\mathbf{p}} e^{i\mathbf{p}\cdot\mathbf{r}}\Pi_{\widetilde{\mathbf{P}}_{\mathbf{p}}}(t)\\ \mathbf{A}(\mathbf{r},t) &= \frac{1}{\sqrt{V}}\sum_{\mathbf{q}} e^{i\mathbf{q}\cdot\mathbf{r}}\mathbf{A}_{\mathbf{q}}(t)\\ \Pi_{\mathbf{A}}(\mathbf{r},t) &= \frac{1}{\sqrt{V}}\sum_{\mathbf{q}} e^{i\mathbf{q}\cdot\mathbf{r}}\Pi_{\mathbf{A}_{\mathbf{q}}}(t),\end{aligned} \tag{C.1}$$

which leads to the Hamiltonian density

$$\mathcal{H}_{PZW} = \sum_{\mathbf{p},\mathbf{q}}\frac{e^{i(\mathbf{p}+\mathbf{q})\cdot\mathbf{r}}}{2V}\left(\underbrace{\frac{\Pi_{\mathbf{A}_{\mathbf{q}}}\Pi_{\mathbf{A}_{\mathbf{p}}}}{\epsilon_0} - \frac{\mathbf{q}\cdot\mathbf{p}\mathbf{A}_{\mathbf{q}}\mathbf{A}_{\mathbf{p}}}{\mu_0}}_{\mathcal{H}_c} + \underbrace{\Pi_{\widetilde{\mathbf{P}}_{\mathbf{p}}}\Pi_{\widetilde{\mathbf{P}}_{\mathbf{q}}} + \omega_{pl,\mathbf{p}}\omega_{pl,\mathbf{q}}\widetilde{\mathbf{P}}_{\mathbf{p}}\widetilde{\mathbf{P}}_{\mathbf{q}}}_{\mathcal{H}_{pl}}\right.$$
$$\left. + \underbrace{\frac{2\Omega_{pl}}{\sqrt{\epsilon_0}}\Pi_{\mathbf{A}_{\mathbf{q}}}\cdot\widetilde{\mathbf{P}}_{\mathbf{p}}}_{\mathcal{H}_{int,1}} + \underbrace{\Omega_{pl}^2\widetilde{\mathbf{P}}_{\mathbf{p}}\cdot\widetilde{\mathbf{P}}_{\mathbf{q}}}_{\mathcal{H}_{int,2}}\right). \tag{C.2}$$

$\mathcal{H}_c$ and $\mathcal{H}_{pl}$ are the free photons and plasmons Hamiltonian densities, while $\mathcal{H}_{int,1}$ is the plasmon–photon (SPP-EC) coupling term, it is responsible for the avoided-crossing behavior and represents the SPP-EC interacting energy density. The term $\mathcal{H}_{int,2}$ is a plasmon self-coupling term, and it represents the plasmons self-coupling energy density.

C.2. Quantizing the fields

Now, by elevating fields and momenta to the role of operators that act on a Hilbert space, we impose the equal-time commutation relations

$$\begin{aligned}\left[\hat{\mathbf{A}}(\mathbf{x}),\hat{\Pi}_{\mathbf{A}}(\mathbf{y})\right] &= \mathrm{i}\hbar\,\delta^3(\mathbf{x}-\mathbf{y})\\ \left[\hat{\tilde{\mathbf{P}}}(\mathbf{x}),\hat{\Pi}_{\tilde{\mathbf{P}}}(\mathbf{y})\right] &= \mathrm{i}\hbar\,\delta^3(\mathbf{x}-\mathbf{y}),\end{aligned} \tag{C.3}$$

while all the other commutators are zero. Then, by introducing appropriate creation (annihilation) operators $\hat{a}^\dagger_{\mathbf{q}}, \hat{b}^\dagger_{\mathbf{p}}$ ($\hat{a}_{\mathbf{q}}, \hat{b}_{\mathbf{p}}$) as

$$\begin{aligned}\hat{\mathbf{A}}_{\mathbf{q}} &= \sqrt{\frac{\hbar}{2\epsilon_0\omega_{\mathrm{c},\mathbf{p}}}}\left(\hat{a}_{\mathbf{q}}+\hat{a}^\dagger_{\mathbf{q}}\right)\\ \hat{\Pi}_{\mathbf{A}_{\mathbf{q}}} &= -\mathrm{i}\sqrt{\frac{\epsilon_0\hbar\omega_{\mathrm{c},\mathbf{q}}}{2}}\left(\hat{a}_{\mathbf{q}}-\hat{a}^\dagger_{\mathbf{q}}\right)\\ \hat{\tilde{\mathbf{P}}}_{\mathbf{p}} &= \sqrt{\frac{\hbar}{2\omega_{\mathrm{pl},\mathbf{p}}}}\left(\hat{b}_{\mathbf{p}}+\hat{b}^\dagger_{\mathbf{p}}\right)\\ \hat{\Pi}_{\tilde{\mathbf{P}}_{\mathbf{p}}} &= -\mathrm{i}\sqrt{\frac{\hbar\omega_{\mathrm{pl},\mathbf{p}}}{2}}\left(\hat{b}_{\mathbf{p}}-\hat{b}^\dagger_{\mathbf{p}}\right),\end{aligned} \tag{C.4}$$

it is possible to verify that equations (C.3) imply the bosonic commutation rules

$$\begin{aligned}\left[\hat{a}_{\mathbf{q}},\hat{a}_{\mathbf{p}}\right] &= \left[\hat{a}^\dagger_{\mathbf{q}},\hat{a}^\dagger_{\mathbf{p}}\right] = 0\\ \left[\hat{b}_{\mathbf{q}},\hat{b}_{\mathbf{p}}\right] &= \left[\hat{b}^\dagger_{\mathbf{q}},\hat{b}^\dagger_{\mathbf{p}}\right] = 0\\ \left[\hat{a}_{\mathbf{q}},\hat{a}^\dagger_{\mathbf{p}}\right] &= \delta_{\mathbf{q},\mathbf{p}}\\ \left[\hat{b}_{\mathbf{q}},\hat{b}^\dagger_{\mathbf{p}}\right] &= \delta_{\mathbf{q},\mathbf{p}}.\end{aligned} \tag{C.5}$$

By plugging equation (C.4) into equation (C.2), exploiting the commutation relations in equation (C.5) and integrating on V, we obtain the total Hamiltonian in the Second Quantization formalism as

$$\begin{aligned}\hat{H}_{\mathrm{PZW}} = \sum_{\mathbf{q}}\Bigg[&\underbrace{\hbar\omega_{\mathrm{c},\mathbf{q}}\left(\hat{a}^\dagger_{\mathbf{q}}\hat{a}_{\mathbf{q}}+\frac{1}{2}\right)}_{\hat{H}_{\mathrm{c}}}+\underbrace{\hbar\omega_{\mathrm{pl},\mathbf{q}}\left(\hat{b}^\dagger_{\mathbf{q}}\hat{b}_{\mathbf{q}}+\frac{1}{2}\right)}_{\hat{H}_{\mathrm{pl}}}\\ &\underbrace{-\mathrm{i}\hbar\gamma\left(\hat{a}_{\mathbf{q}}-\hat{a}^\dagger_{\mathbf{q}}\right)\left(\hat{b}_{-\mathbf{q}}+\hat{b}^\dagger_{-\mathbf{q}}\right)}_{\hat{H}_{\mathrm{int},1}}+\underbrace{\hbar\delta\left(\hat{b}_{\mathbf{q}}+\hat{b}^\dagger_{\mathbf{q}}\right)\left(\hat{b}_{-\mathbf{q}}+\hat{b}^\dagger_{-\mathbf{q}}\right)}_{\hat{H}_{\mathrm{int},2}}\Bigg],\end{aligned} \tag{C.6}$$

where

$$\gamma = \frac{\Omega_{\mathrm{pl}}}{2}\sqrt{\frac{\omega_{\mathrm{c},\mathbf{q}}}{\omega_{\mathrm{pl},\mathbf{q}}}},\quad \delta = \frac{\Omega^2_{\mathrm{pl}}}{2\omega_{\mathrm{pl},\mathbf{q}}}. \tag{C.7}$$

ORCID iD

Marco Vallone https://orcid.org/0000-0003-3392-1810

References

[1] Peskin M E and Schroeder D V 1995 *Quantum Field Theory* (CRC Press)
[2] Cohen-Tannoudji C, Dupont-Roc J and Grynberg G 1997 *Photons and Atoms: Introduction to Quantum Electrodynamics* (Wiley)
[3] Jaynes E T and Cummings F W 1963 *Proc. IEEE* **51** 89–109
[4] Hümmer T, García-Vidal F J, Martín-Moreno L and Zueco D 2013 *Phys. Rev. B* **87** 115419
[5] Liu J and Li Z Y 2014 *Opt. Express* **22** 28671–82
[6] Larson J and Mavrogordatos T 2024 *The Jaynes–Cummings Model and its Descendants (2nd edition): Modern Research Directions* (IOP Publishing)
[7] Rabi I I 1936 *Phys. Rev.* **49** 324–8

[8] Rabi I I 1937 *Phys. Rev.* **51** 652–4
[9] Wang B, Yu P, Wang W, Zhang X, Kuo H C, Xu H and Wang Z M 2021 *Adv. Opt. Mater.* **9** 2001520
[10] Gerry C C 1988 *Phys. Rev. A* **37** 2683–6
[11] Valle E D, Zippilli S, Laussy F P, Gonzalez-Tudela A, Morigi G and Tejedor C 1988 *Phys. Rev. B* **81** 035302
[12] Scala G, Słowik K, Facchi P, Pascazio S and Pepe F V 2021 *Phys. Rev. A* **1** 013722
[13] Todorov Y, Andrews A M, Colombelli R, Liberato S D, Ciuti C, Klang P, Strasser G and Sirtori C 2010 *Phys. Rev. Lett.* **105** 196402
[14] Forn-Díaz P, Lamata L, Rico E, Kono J and Solano E 2019 *Rev. Mod. Phys.* **2** 025005
[15] Kockum A F, Miranowicz A, Liberato S D, Savasta S and Nori F 2019 *Nat. Rev. Phys.* **1** 19–40
[16] Baranov D G, Munkhbat B, Zhukova E, Bisht A, Canales A, Rousseaux B, Johansson G, Antosiewicz T J and Shegai T 2020 *Nat. Commun.* **11** 2715
[17] Wang Z, Li L, Wei S, Shi X, Xiao J, Guo Z, Wang W, Wang Y and Wang W 2023 *J. Appl. Phys.* **133** 063101
[18] Rosenberg J, Shenoi R V, Krishna S and Painter O 2010 *Opt. Express* **18** 3672–86
[19] Tong J, Tobing L Y M, Qiu S, Zhang D H and Perera A G U 2018 *Appl. Phys. Lett.* **113** 011110
[20] Tappura K 2018 *MDPI Proc.* **2** 1063
[21] Vanamala N, Santiago K C and Das N C 2019 *AIP Adv.* **9** 025113
[22] Budhu J, Pfiester N, Choi K K, Young S, Ball C, Krishna S and Grbic A 2021 *IEEE Trans. Antennas Propagation* **69** 6762–71
[23] Zhang G, Xu C, Sun D, Wang Q, Lu G and Gong Q 2024 *Fundam. Res.* (https://doi.org/10.1016/j.fmre.2024.01.002)
[24] Sarkar S and König T A F 2024 *Adv. Sens. Res.* **1** 2300054
[25] Ai B, Fan Z and Wong Z J 2024 *Microsyst. Nanoeng.* **1** 5
[26] Greffet J J 2012 Introduction to Surface Plasmon Theory *Plasmonics* vol 167 ed S Enoch and N Bonod (Springer) pp 105–48
[27] Raether H 1988 *Surface plasmons on smooth and rough surfaces and on gratings* (*Springer Tracts in Modern Physics* vol 111) (Springer)
[28] Han Z and Bozhevolnyi S I 2013 *Rep. Prog. Phys.* **76** 016402
[29] Vallone M, Goano M and Tibaldi A 2024 *Opt. Express* **32** 27536–51
[30] Miller S E 1954 *Bell Syst. Tech. J.* **33** 661–719
[31] Pierce J R 1954 *J. Appl. Phys.* **25** 179–83
[32] Gould R W 1955 *IEEE Trans. Electron Devices* **2** 37–42
[33] Törmä P and Barnes W L 2015 *Rep. Prog. Phys.* **78** 013901
[34] Groesen E V 1998 *Opt. Quantum Electron.* **30** 467–74
[35] Todorov Y and Sirtori C 2012 *Phys. Rev. B* **85** 045304
[36] Mueller N S, Okamura Y, Vieira B G M, Juergensen S, Lange H, Barros E B, Schulz F and Reich S 2020 *Nature* **583** 780
[37] Salmon W, Gustin C, Settineri A, Stefano O D, Zueco D, Savasta S, Nori F and Hughes S 2022 *Nanophoton* **11** 1573–90
[38] Power E A and Zienau S 1957 *Nuovo Cimento* **6** 7–17
[39] Woolley R G and Coulson C A 1971 *Proc. R. Soc. A* **321** 557–72
[40] Rousseau E and Felbacq D 2017 *Sci. Rep.* **7** 11115
[41] Rouse D M, Lovett B W, Gauger E M and Westerberg N 2021 *Sci. Rep.* **11** 4281
[42] Vukics A, Konya G and Domokos P 2021 *Sci. Rep.* **11** 16337
[43] Settineri A, Stefano O D, Zueco D, Hughes S, Savasta S and Nori F 2021 *Phys. Rev. Res.* **3** 023079
[44] Andrews D L, Bradshaw D S, Forbes K A and Salam A 2020 *J. Opt. Soc. Am. B* **37** 1153–72
[45] Mahan G D 2000 *Many-Particle Physics* 3rd edn (Kluwer Academic Publishers)
[46] Coleman P 2011 *Introduction to Many-Body Physics* (Cambridge University Press)
[47] Goldstein H, Poole C and Safko J 2001 *Classical Mechanics* 3rd edn (Addison-Wesley)
[48] Orfanidis S J 2016 Electromagnetic waves and antennas (available at: https://www.ece.rutgers.edu/orfanidis)
[49] Jackson J D 1999 *Classical Electrodynamics* 3rd edn (Wiley)
[50] Cohen-Tannoudji C, Diu B and Laloë F 1977 *Quantum Mechanics* (Wiley)
[51] Andrews D L, Jones G A, Salam A and Woolley R G 2018 *J. Comput. Phys.* **148** 040901
[52] Dicke R H 1954 *Phys. Rev.* **93** 99–110
[53] Hopfield J J 1958 *Phys. Rev.* **112** 1555–67
[54] Mattuck R D 1976 *A Guide to Feynman Diagrams in the Many-Body Problem* 2nd edn (McGraw-Hill)
[55] Vallone M, Goano M, Hanna S, Figgemeier H, Eich D, Bertazzi F and Tibaldi A 2025 Plasmonics: a path towards HOT infrared detectors *Proc. SPIE* **13360** 1336005
[56] You C, Nellikka A C, Leon I D and Magaña-Loaiza O S 2020 *Nat. Photon.* **9** 1243–69
[57] Yoo D, de León-Pérez F, Lee I H, Mohr D A, Raschke M B, Caldwell J D, Martín-Moreno L and Oh S H 2021 *Nat. Photon.* **15** 125–30
[58] Pisani F, Gacemi D, Vasanelli A, Li L, Davies A G, Linfield E, Sirtori C and Todorov Y 2023 *Nat. Commun.* **14** 3914
[59] Liberato S D and Ciuti C 2009 *Phys. Rev. Lett.* **102** 136403
[60] Vasanelli A, Todorov Y and Sirtori C 2016 *C. R. Phys.* **17** 861–73
[61] Vigneron P B, Pirotta S, Carusotto I, Tran N L, Biasiol G, Manceau J M, Bousseksou A and Colombelli R 2019 *Appl. Phys. Lett.* **114** 131104
[62] Rousseaux B, Todorov Y, Vasanelli A and Sirtori C 2023 *Phys. Rev. B* **108** 125417
[63] Cerisola F, Berritta M, Scali S, Horsley S A R, Cresser J D and Anders J 2024 *New J. Phys.* **26** 053032
[64] Shokova M A and Bochenkov V E 2021 *Nanomaterials* **11** 3334
[65] Mirzaei-Ghormish S, Qaderi K and Smalley D 2024 *Sci. Rep.* **14** 12607
[66] Chu S *et al* 2014 *ACS Photonics* **1** 32–37
[67] Cao E, Lin W, Sun M, Liang W and Song Y 2018 *ACS Photonics* **7** 145–67
[68] Binder K and Young A P 1986 *Rev. Mod. Phys.* **58** 801–976
[69] Hosseinabadi H, Chang D E and Marino J 2024 *Phys. Rev. Res.* **6** 043314
[70] Hosseinabadi H, Chang D E and Marino J 2024 *Phys. Rev. Res.* **6** 043313